Research Square

Preprints are preliminary reports that have not undergone peer review.
They should not be considered conclusive, used to inform clinical practice,
or referenced by the media as validated information.

Compact representation of material-state fields in dexel-based virtual manufacturing of hybrid components

Mariem Ben Salem

bensalem@ifw.uni-hannover.de

Leibniz University Hannover

Volker Böß

Leibniz University Hannover

Klaas Maximilian Heide

Leibniz University Hannover

Research Article

Keywords: additive manufacturing, dexel model, material-state representation, data compression, virtual manufacturing

Posted Date: November 24th, 2026

DOI: https://doi.org/10.21203/rs.3.rs-11732711/v1

License: This work is licensed under a Creative Commons Attribution 4.0 International License.
Read Full License

Additional Declarations: No competing interests reported.

Compact representation of material-state fields in dexel-based virtual manufacturing of hybrid components

Keywords: additive manufacturing; dexel model; material-state representation; data compression; virtual manufacturing

Abstract

Virtual manufacturing of components with locally varying material compositions requires the representation of material states that vary along the component. These states include quantities such as residual stresses, microstructure, and hardness. Finite element simulations can resolve these states, but they become too costly at full component scale. Existing approaches are therefore limited to local process regions. This work presents a method for storing material-state information in a dexel-based representation. The material-state data are encoded as parametric functions along the build direction, reducing data volume and memory requirements. The approach is demonstrated using temperature data obtained from a voxel-based thermal simulation, with B-splines used as a representative function class. Applied to one-dimensional temperature profiles, the method achieves a reduction of 84 % in stored data at a maximum RMSD of 0.1 % of the peak temperature. The proposed method enables an efficient and scalable representation of heterogeneous material states and provides a foundation for property-aware virtual manufacturing and process planning of hybrid structures.

1. Introduction

Hybrid components produced by additive manufacturing processes combine dense structural regions with controlled-porosity zones and graded material compositions within a single part [1, 2]. The defining characteristic of such components, and the central challenge addressed in this work, is that their material state varies continuously across the entire component volume. Quantities such as local density, microstructural composition, and residual stress are not uniform. They change from region to region as a direct consequence of the heterogeneous internal architecture and the spatially varying process conditions during deposition [1]. For virtual manufacturing and process planning of these components, it is therefore necessary to describe and store the material state across the entire component geometry rather than only locally within individual process zones.

Simulation of material state in additive manufacturing processes is predominantly based on the Finite Element Method (FEM), in which the workpiece is discretized into volume elements such as tetrahedra or hexahedra [3]. Thermo-mechanically coupled FEM models are well established for predicting local temperature fields, residual stresses, and distortion during deposition [3, 4]. However, FEM-based simulations require resolving all state variables throughout the entire three-dimensional domain, which leads to high memory consumption and computation time that scale poorly with component size [3, 5]. As a consequence, FEM-based simulations of AM processes are typically restricted to local build regions, individual tracks, or small representative subdomains [3]. For hybrid components spanning centimeter- to decimeter-scale geometries, obtaining a component-wide description of the resulting material state using FEM becomes computationally impractical.

From a virtual manufacturing perspective, dexel-based geometric representations offer a well-established and scalable alternative for simulating evolving part geometries at component scale [6, 7]. In dexel models, the workpiece is represented as a structured grid of parallel line segments, each encoding material occupancy along its depth direction through interval lists [6]. This architecture enables efficient Boolean operations for material deposition and removal, and has been applied to the geometric simulation of DED and hybrid additive-subtractive processes at scales that are computationally prohibitive for volumetric FEM models [6, 7]. However, across all of these approaches, the dexel remains a purely geometric descriptor: it stores interval boundaries that indicate where

material is present or absent, but carries no information about the local material state, such as density gradients, residual stress distribution, or temperature history, along its depth [6]. Spatially varying material states in hybrid components are therefore not captured by existing dexel-based virtual manufacturing models.

Consequently, a representational gap exists between the two available classes of simulation tools: FEM models resolve material-state variables accurately but do not scale well to component scale, whereas dexel-based models scale efficiently to large parts but represent only geometry rather than material state. For hybrid components, neither class alone is sufficient. What is missing is a representation that combines the geometric scalability of dexel models with the ability to store and access spatially resolved material-property information along each dexel depth at component scale while maintaining manageable memory requirements.

To address this gap, this work presents a method for representing material-state distributions in a compact form suitable for component-scale virtual manufacturing. Instead of storing sampled fields obtained from voxel-based or FEM simulations, the spatial distribution of material states is encoded as compact parametric functions along the build direction. These representations can be stored efficiently within a dexel-based virtual manufacturing model while preserving essential gradients and transitions of the material state. To demonstrate the data efficiency of the approach, temperature profiles obtained from voxel-based thermal simulations are approximated using B-splines as a representative function class [8]. The proposed method provides a scalable representation of spatially varying material states and forms a foundation for property-aware virtual manufacturing and process planning of hybrid components.

2. Methodology

The proposed methodology is based on a functional representation of spatially varying material-state fields along dexels. The underlying concept of this representation is detailed in Section 2.1, while its application to a representative dataset and the corresponding study setup are described in Section 2.2.

2.1. Functional representation of material-state fields in dexel models

The proposed method aims at representing spatially varying material-state fields in a compact form that is compatible with dexel-based virtual manufacturing models.

In a dexel representation, the component is described by a structured grid in the lateral directions *(x, y)*, where each grid position corresponds to one dexel. A dexel consists of one or more line segments along a predefined depth direction *z*, defined by start and end points that describe the material occupancy.

The central idea of the proposed method is to associate each dexel with a continuous function describing the material-state distribution along its depth direction. Figure 1 illustrates the dexel-based representation and the association of the functional material-state description with the dexel segments.

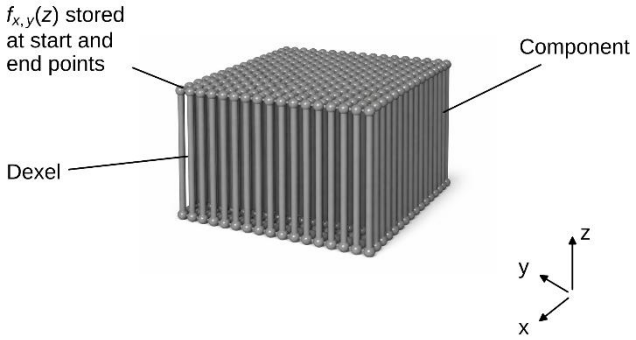


Fig. 1 Dexel-based representation of a component. The geometry is discretized on a structured *(x,y)*-grid, where each grid position corresponds to a dexel

Instead of storing discrete samples of a scalar field, such as temperature or residual stress, the field is represented by a parametric function $f_{x,y}(z)$ for each lateral position *(x, y)*. This function provides the material-state value at any depth position *z* within the corresponding dexel segment. The representation is independent of the underlying simulation method used to obtain the data. It can be applied to scalar fields originating from FEM, voxel-based simulations, or experimental measurements. Likewise, the choice of the function class is not restricted; any suitable parametric representation can be employed, provided that it allows accurate reconstruction of the field with a reduced number of parameters. Within the dexel model, the parameters defining $f_{x,y}(z)$ are stored as attributes associated with the corresponding dexel segments. Since the dexels are organized on a structured *(x, y)*-grid, the spatial assignment between geometry and material-state representation is defined implicitly by this indexing. This approach transforms the dexel from a purely geometric representation into a property-resolved representation, enabling efficient storage and evaluation of spatially varying material states at component scale.

2.2. Study setup and application to voxel-based temperature data

To evaluate the proposed representation, it is applied to a scalar temperature field obtained from a voxel-based thermal simulation. The dataset consists of a three-dimensional field $T(x,y,z)$ defined on a regular grid with dimensions $N_x \times N_y \times N_z$. For each lateral position *(x,y)*, the field is interpreted as a one-dimensional profile along the depth direction:

$$T_{x,y}(z_i), i = 1, \dots, N_z \tag{1}$$

These profiles serve as input for the functional representation. The dataset used in this study contains N_x = 207, N_y = 207, and N_z = 141 voxels, corresponding to approximately 6.0 million scalar values. The voxel edge length is 5 µm. The temperature field results from a thermal simulation of Ti6Al4V with a laser power of 100 W, a scan speed of 1.0 m/s and a laser radius of 26 µm. The temperature field represents a single time instance of a laser powder bed fusion (PBF-LB) process and exhibits both steep local gradients in the melt pool region and slowly varying regions elsewhere. This combination provides a demanding test case for the functional approximation. For the present study, B-splines are used as a representative function class to approximate the profiles. The splines are fitted with the make_splrep routine of SciPy [9], which implements the FITPACK algorithm [8]. The choice is motivated by their flexibility and local support; however, the proposed method is not restricted to this representation and can be applied to other suitable function classes. Each profile is approximated by a function $S_{x,y}(z)$, obtained by minimizing the deviation to the original data under a prescribed root-mean-square deviation (RMSD). The fitting procedure is based on the condition

$$\sum_i \left[T_{x,y}(z_i) - S_{x,y}(z_i)\right]^2 \leq s \tag{2}$$

where s is the smoothing parameter. The RMSD is defined as

$$RMSD = \sqrt{\frac{1}{N_z} \cdot \sum_i \left[T_{x,y}(z_i) - S_{x,y}(z_i)\right]^2} \tag{3}$$

and is controlled via the parameter ρ, with

$$s = \rho^2 \cdot N_z \tag{4}$$

Thus, ρ directly specifies the target approximation accuracy in physical units. Each function is described by a set of parameters, including both knot locations and corresponding coefficients. These parameters define the complete functional representation and are used to evaluate the storage requirements of the method. The trade-off between approximation accuracy and data reduction is analyzed in Section 3.

3. Results and Discussion

This section presents the results of applying the B-spline approximation to the full thermal dataset described in Section 2.2. Section 3.1 examines the approximation behavior on the most demanding individual profile in the dataset, illustrating how the fit quality and residual distribution depend on the choice of ρ. Section 3.2 reports the global compression performance across all profiles and characterizes the accuracy-compression trade-off as a function of ρ.

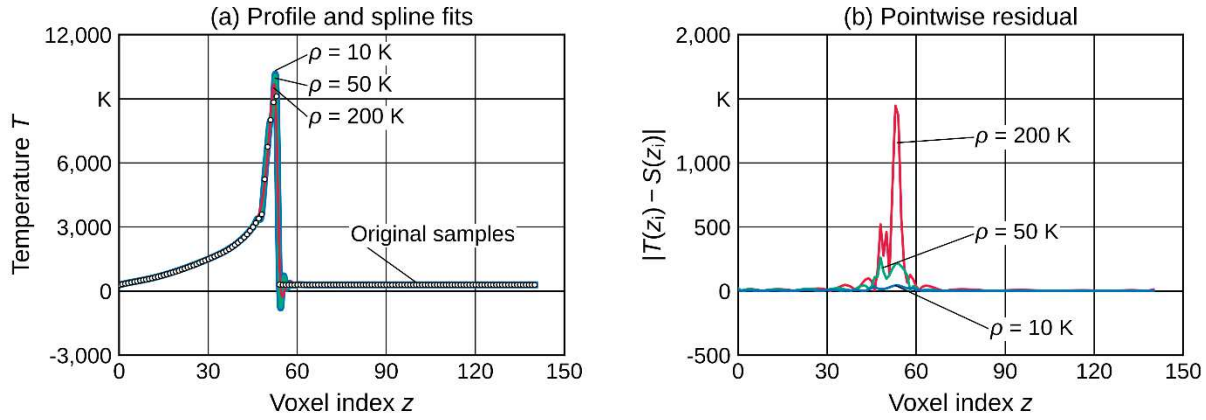
3.1. Approximation of the Worst-Case Temperature Profile

To illustrate the behavior of the fitting procedure, the approximation is first evaluated for the profile of maximum temperature in the dataset. This profile contains the steepest gradient in the entire field, located at the melt pool region near voxel index z = 53, and therefore represents the most demanding case for the spline fitting. It should be noted that the peak temperature of 9,124 K in the dataset exceeds physically realistic values for Ti6Al4V. This is a known artifact of the discretization of the Gaussian heat source on a coarse voxel grid, where the concentrated energy input is distributed over a finite cell volume, leading to locally elevated temperatures. The peak value is retained here without modification, as it represents the most demanding test case for the approximation and does not affect the validity of the compression results.

Each B-spline $S(z)$ is fully described by two sets of parameters, the knot vector $t = (t_0, t_1, \ldots, t_{n_knots-1})$ and the spline coefficients $c = (c_0, c_1, \ldots, c_{n_coeffs-1})$, together with the polynomial degree k = 5. These parameters together define the complete functional representation stored per dexel. The number of knots and coefficients is determined adaptively by the fitting algorithm for each profile, depending on the prescribed smoothing parameter s.

Figure 2 shows the approximation results for three representative values of ρ. In Fig. 2a, the original voxel samples and the fitted splines are shown. At all three values of ρ, the spline captures the overall shape of the profile. The pointwise residuals in Fig. 2b reveal the differences more clearly: at ρ = 10 K, the maximum residual at the steep peak remains below 44 K, while at ρ = 50 K and ρ = 200 K it reaches approximately 260 K and 1,446 K, respectively. These values represent local peak residuals at a single point. The RMSD, which is averaged over all N_z points, equals the respective ρ value in all three cases. In all three cases, the residuals are negligible outside the peak region, confirming that the approximation error is strongly localized at the steep melt-pool gradient. This behavior reflects the

adaptive nature of the knot selection: more knots are allocated where the gradient is steepest, and fewer where the profile varies slowly.



Simulation and process parameters

Laser power: 100 W
Scan speed: 1.0 m/s
Laser radius: 26 µm
Powder bed thickness: 30 µm
Material: Ti6Al4V
Exposure strategy: filling

Fig. 2 B-spline approximation of the worst-case temperature profile for three values of ρ. (a) Original voxel samples and spline fits. (b) Pointwise residual

3.2. Global Compression Performance

The B-spline approximation is applied to all *(x, y)* profiles in the dataset for values of ρ ranging from 1 K to 300 K. The upper bound of 300 K corresponds to approximately 3 % of the peak temperature, providing a physically meaningful limit beyond which the approximation error would become significant relative to the temperature range of the process. Note that ρ defines an upper bound on the RMSD. The fitting algorithm adaptively selects the number of knots such that the achieved RMSD does not exceed ρ. For a few values of ρ, the iteration does not converge for one to three of the 42,849 profiles. Their RMSD then exceeds ρ, which causes the steps in the maximum RMSD curve in Fig. 4.

The total data volume of the original voxel representation is:

$$\boldsymbol{N_{voxel} = N_x \times N_y \times N_z = 207 \times 207 \times 141 = 6,041,709 \text{ values}} \tag{5}$$

For the B-spline representation, the total number of stored parameters across all profiles is:

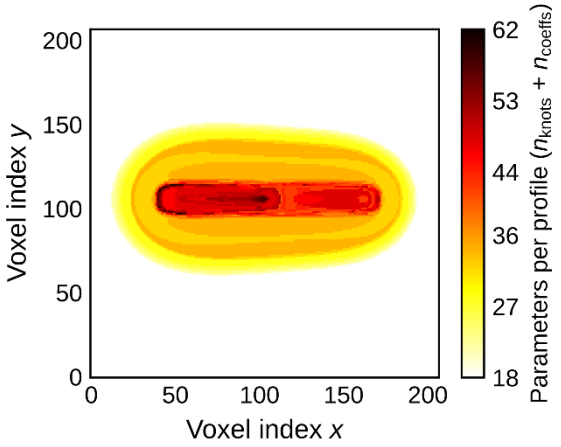
$$\boldsymbol{P_{total} = \sum_{(x,y)} [n_{knots(x,y)} + n_{coeffs(x,y)}]} \tag{6}$$

where $n_{knots(x,y)}$ and $n_{coeffs(x,y)}$ denote the number of knot vector entries and spline coefficients for the profile at lateral position *(x, y)*, respectively. The global compression ratio is then defined as:

$$\boldsymbol{C_{global} = \frac{N_{voxel}}{P_{total}}} \tag{7}$$

The spatial distribution of parameter counts across the component cross-section at ρ = 10 K is shown in Fig. 3. Profiles at positions where the temperature passes through the melt pool region along *z* require more parameters to satisfy the prescribed tolerance, while the majority of the cross-section is

represented with far fewer parameters. This non-uniform distribution confirms that the fitting adapts automatically to local profile complexity.

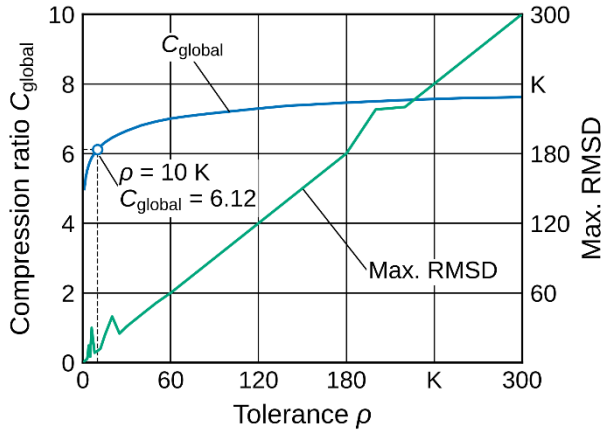


Simulation and process parameters

Laser power: 100 W	Powder bed thickness: 30 µm
Scan speed: 1.0 m/s	Material: Ti6Al4V
Laser radius: 26 µm	Exposure strategy: filling

Fig. 3 Spatial distribution of B-spline parameter count per profile over the component cross-section at ρ = 10 K

Figure 4 shows C_{global} and the maximum RMSD across all profiles as a function of ρ. The maximum RMSD is defined as the largest RMSD value observed across all *(x, y)* profiles, representing the worst-case approximation error. Even at the tightest tolerance tested (ρ = 1 K), a global compression ratio of $C_{global} \approx 5.0$ is achieved, corresponding to a reduction of approximately 80 % in stored scalar values.



Simulation and process parameters

Laser power: 100 W	Powder bed thickness: 30 µm
Scan speed: 1.0 m/s	Material: Ti6Al4V
Laser radius: 26 µm	Exposure strategy: filling

Fig. 4 Global compression ratio C_{global} and maximum RMSD as a function of the tolerance ρ

A value of ρ = 10 K is selected as the operating point for the following reasons. As shown in Fig. 2b, the spline fit at this tolerance captures the profile shape accurately, with a maximum local residual below 44 K confined to the steepest part of the melt-pool peak. Outside this region, the residuals are negligible. At the same time, ρ = 10 K corresponds to 0.1 % of the peak temperature of 9,124 K in the dataset, confirming that the worst-case approximation error remains negligible relative to the full temperature range of the process. At ρ = 10 K, a global compression ratio of C_{global} = 6.1 is achieved, corresponding to a reduction of approximately 84 % in stored scalar values. The maximum RMSD across all profiles at this operating point is 10.0 K. Table 1 summarizes the data-volume comparison at this operating point.

Metric	Voxel	B-spline	C_{global}
Total stored scalar values	6,041,709	987,438	6.12
Values per profile	141	23 (avg.)	—
RMSD max. (K)	—	10.0	—

Table 1 Data-volume comparison between the voxel representation and the B-spline representation at ρ = 10 K

The parametric study demonstrates that ρ provides direct, interpretable control over the accuracy-compression trade-off. More generally, the method is not restricted to temperature fields: any scalar material-state field, such as density or residual stress, can be represented in the same way, with ρ defined in the corresponding physical unit and chosen independently for each field.

A limitation of this study is that the demonstration is based on a single time instance of a single simulation dataset. The compression ratio will vary with process parameters and component geometry, and the chosen dataset represents one, arguably demanding, realization of the thermal field structure. Future work should evaluate the method across multiple time instances and process conditions to establish the generality of the compression performance reported here.

4. Conclusion

This paper has introduced a method for the compact representation of material-state fields in additive manufacturing components, based on the association of parametric functions with dexel segments, demonstrated using B-spline approximation of voxel-based temperature profiles. Each column profile is approximated by a B-spline, replacing N_z voxel samples with $n_{knots} + n_{coeffs}$ spline parameters. Applied to a thermal dataset of 207 × 207 × 141 voxels, the method reduces the stored scalar values by 84 % at a maximum RMSD of 10 K, corresponding to 0.1 % of the peak temperature, demonstrating that the compact functional description captures the essential information of the original field at a fraction of the storage cost.

The significance of this result is twofold. First, it demonstrates that spatially varying material-state fields can be represented compactly in a form that is compatible with dexel-based virtual manufacturing models, without prohibitive storage overhead. Second, it establishes B-spline approximation as a principled and efficient mechanism for this purpose: the target tolerance ρ, which defines an upper bound on the RMSD, provides direct, interpretable control over the accuracy-compression trade-off and can be selected independently for each material-state field.

Future work will demonstrate the full integration of the proposed representation within a dexel-based process simulation, extend the evaluation to additional material-state fields such as density and residual stress, and validate the method on simulation data from different additive processes and component geometries.

References

[1] Svetlizky D, Zheng B, Vyatskikh A, Das M, Bose S, Bandyopadhyay A, Schoenung JM, Lavernia EJ, Eliaz N (2022) Laser-based directed energy deposition (DED-LB) of advanced materials. Mater Sci Eng A 840:142967. https://doi.org/10.1016/j.msea.2022.142967

[2] Li K, Zhang M, Zhang Z, Jin P, Wang Y, Yan W, Zhu L, Zhang DZ, Murr LE (2025) High performance realization of functionally graded materials based on integrated optimal design and additive manufacturing: a review. Int Mater Rev 70:497–547. https://doi.org/10.1177/09506608251354889

[3] Bayat M, Dong W, Thorborg J, To AC, Hattel JH (2021) A review of multi-scale and multi-physics simulations of metal additive manufacturing processes with focus on modeling strategies. Addit Manuf 47:102278. https://doi.org/10.1016/j.addma.2021.102278

[4] Chiumenti M, Cervera M, Salmi A, Agelet de Saracibar C, Dialami N, Matsui K (2010) Finite element modeling of multi-pass welding and shaped metal deposition processes. Comput Methods Appl Mech Eng 199:2343–2359. https://doi.org/10.1016/j.cma.2010.02.018

[5] Afrasiabi M, Bambach M (2023) Modelling and simulation of metal additive manufacturing processes with particle methods: a review. Virtual Phys Prototyp 18(1). https://doi.org/10.1080/17452759.2023.2274494

[6] Böß V, Denkena B, Dittrich M-A, Malek T, Friebe S (2021) Dexel-based simulation of directed energy deposition additive manufacturing. J Manuf Mater Process 5:9. https://doi.org/10.3390/jmmp5010009

[7] Sun Y-J, Yan C, Wu S-W, Gong H, Lee C-H (2018) Geometric simulation of 5-axis hybrid additive-subtractive manufacturing based on Tri-dexel model. Int J Adv Manuf Technol 99:2597–2610. https://doi.org/10.1007/s00170-018-2577-6

[8] Dierckx P (1993) Curve and surface fitting with splines. Oxford University Press, Oxford

[9] Virtanen P, Gommers R, Oliphant TE et al (2020) SciPy 1.0: fundamental algorithms for scientific computing in Python. Nat Methods 17:261–272. https://doi.org/10.1038/s41592-019-0686-2